Spontaneous pulsations in gas class-A lasers with weakly anisotropic cavities

L. P. Svirina, V. G. Gudelev, and Yu. P. Zhurik
Institute of Physics, Academy of Sciences of Belarus, Skaryna Avenue 70, Minsk 220072, Belarus
(Received 23 January 1997; revised manuscript received 14 August 1997)

Spontaneous pulsations and polarization multistability resulting from the nonlinear interaction of two standing waves with an active medium in a single-longitudinal-mode Fabry-Pérot gas laser with a weakly anisotropic cavity have been studied at different cavity anisotropies and different transitions between the working levels with and without an axial magnetic field applied to the active medium. As predicted theoretically, a series of polarization dynamical phenomena have been observed experimentally in the He-Ne ($\lambda = 1.15\ \mu$m) laser in the case of orthogonal elliptically polarized eigenstates of the cavity. Periodic oscillations of two qualitatively different forms (distorted sinusoids and large spikes), the transition between two stationary orthogonal elliptically polarized waves in the vicinity of the line center tuning which occurs through the region with polarization instability, as well as switches between the orthogonally polarized components when the output is nonstationary have been found. It is shown that the diversity of nonstationary polarization phenomena in gas lasers with weakly anisotropic cavities is due to spontaneous pulsations of intensities, ellipticities, and azimuths of two emitted waves, caused by the competition of the nonlinear active medium and empty cavity anisotropies. The results of the theoretical modeling are in quantitative agreement with the experimental results. [S1050-2947(97)00912-8]

PACS number(s): 42.60.Mi, 42.65.Sf

I. INTRODUCTION

In the last few years, polarization dynamical phenomena have been studied intensively in different laser systems of which gas lasers with anisotropic cavities, where instabilities have been known from the beginning of the laser age [1–4], play an important part [5–16,18–23]. Gas lasers represent an ideal model for theory, where different approaches have been developed, and for experiment because they offer wide possibilities for controlling the nonlinear interaction of the emitted field with the active medium, the empty cavity parameters, and external fields, i.e., all those factors which determine the state of polarization of laser output [4].

Up to now two different approaches have been known in the theory of gas (class-A) lasers with anisotropic cavities: one of them is based on the vectorial extension of the Lamb scalar theory [24] and the other one on the Jones vectors and matrices formalism [25,26]. Both of them are valid in the third order of the field perturbation theory at adiabatical elimination of the dynamics of atomic and material variables.

The first approach holds in two limiting cases: when the anisotropy of the empty cavity is much less (or equal to zero) than the anisotropy of the active medium (see, for example, [27–30,14]) and when the cavity anisotropy is much higher than the medium anisotropy (see, for example, [31,32]). In the first case, polarization of the emitted field is governed mainly (or fully) by the active medium, and the empty cavity anisotropy is undertaken as a small addition to the medium anisotropy, uniformly spread over the cavity length. This case can be regarded as ''a laser with nearly, slightly anisotropic, quasi-isotropic cavity'' (or isotropic cavity). Here the anisotropy of the cavity is too small compared with the anisotropy of the medium (or equal to zero). In the second case, polarization of the emitted field is determined mainly by the empty cavity, and the anisotropy of the active medium is undertaken as a small addition to the cavity anisotropy, uniformly spread over the cavity length [32]. This case can be regarded as ''a laser with strongly anisotropic cavity.''

The main advantage of the second approach, based on the matrix formalism, is the possibility to take into account the disposition of the anisotropic elements and active medium in the cavity and to follow sequentially the evolution of the state of polarization of the emitted field from point to point of the cavity. The Jones vector of the emitted wave with arbitrary polarization as well as the Jones matrices of the active medium and empty cavity, having different eigenstates in the general case, are represented in one Cartesian basis. This provides the fulfillment of the self-consistency condition with respect to the polarization parameters. In the so-called ''laser with weakly anisotropic cavity,'' both the cavity and the active medium equally influence the state of polarization of the emitted field. If the emitted field polarization at any point of the cavity is reproduced during one round-trip (stationary operation) or a few round-trips (self-pulsing regime) the notion ''laser eigenstates'' has meaning. For details see [34,15,16].

Recently [8,33] a model has been developed of a single-mode (one-frequency) gas laser which is valid in the third-order field approximation, where the deformation of the state of polarization of the electromagnetic field from point to point of the cavity is taken into account through the coordinate derivatives: non-mean-field theory.

A radically new theoretical approach based on [17] has been developed in [5–7] to study polarization dynamical phenomena in high gain gas lasers. This approach is beyond the scope of Lamb's third-order approximation, and includes the dynamics of atomic and material variables (class-C laser).

A large number of polarization dynamical phenomena such as polarization hysteresis and bistability, rotation of the electromagnetic wave azimuth, and polarization switches, have been found in gas class-A lasers with anisotropic cavi-

ties and explained within the framework of the vectorial extension of Lamb's approach (see, for example, [27–30,35–38,14]).

The interest in such lasers has been renewed due to the experimental observation of the nonstationary behavior of polarization parameters without any external time-dependent influence (polarization instability) which cannot be explained in the framework of Lamb's approach (see, for example, [14]).

These phenomena are known to be present in the He-Ne laser at the $j_b=1\rightarrow j_a=2$ [9,10] and in the He-Xe [10] laser at the $j_b=3\rightarrow j_a=2$ transition with linear phase anisotropy of the cavity as well as in the He-Ne [11] laser at the $j_b=1\rightarrow j_a=1$ transition and circular phase anisotropy of the cavity.

Experimentally, polarization instability phenomena manifested themselves as two types of transitions between the steady orthogonal states of polarization (through polarization instability, registered as azimuth rotation, and through bistability) observed in the vicinity of the line center tuning at linearly and circularly polarized eigenstates of the empty cavity [9,11] as well as in periodical oscillations of orthogonal components of the laser output, which have the form of distorted sinusoids and large spikes observed in [10].

Theoretically, polarization instabilities were predicted in [17,5–7], in [8], and in [15,16]. In the first series of works which are valid for the neutral homogeneously broadened $j_b=1\rightarrow j_a=0$ transition, polarization instabilities are due to the inclusion of the dynamics of material and atomic variables. A large number of new polarization dynamical phenomena were predicted in [5,6] and the experimentally observed polarization switches of linearly and circularly polarized waves have been explained in [7].

In [8], the experimental results pointing to the nonstationary behavior of polarization parameters in the Faraday gas laser [1–3,39] at the $j\rightarrow j+1$ transition have been explained qualitatively from the viewpoint of the single-mode (one-frequency) model. The results of [8] in the absence of amplitude anisotropy in the cavity are in agreement with those obtained on the basis of the matrix approach in [15] (item 4).

In the third series of works, which are based on the matrix approach, polarization instabilities arise in the case where the active medium and empty cavity anisotropies are comparable in values (weakly anisotropic cavities). In this case the state of polarization of the emitted field is governed equally by the cavity and medium anisotropies. Thus polarization instabilities are due to the competition of these anisotropies.

In Ref. [16], a mathematical model was developed of a single-longitudinal-mode (two-frequency) gas laser with an arbitrary value and type of cavity anisotropy for arbitrary transitions between the working levels with a longitudinal magnetic field imposed on the active medium. In the case of a weakly anisotropic cavity having linear phase anisotropy at the $j\rightarrow j+1$ transitions polarization instability was found. It appears as spontaneous pulsations of intensities, ellipticities, and azimuths of two emitted waves and is due to the instability of steady states of polarization parameters of the field. Two types of transitions, observed experimentally in the vicinity of the line center tuning in [9], were discovered. Polarization multistability was predicted.

The present work is to answer the following questions.

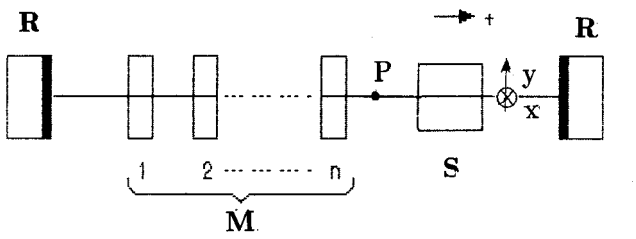

FIG. 1. The schematical representation of the anisotropic-cavity gas laser: R are the mirrors, S is the active medium, M is the anisotropic elements.

(1) What other laser systems besides those with linearly [9,10,16] and circularly [11] polarized eigenstates of the empty cavity can exhibit polarization instability?

(2) Is there a connection between the periodic oscillations of orthogonal components of the output in the form of distorted sinusoids and large spikes observed experimentally in [10] and spontaneous pulsations of the characteristics of two emitted waves predicted in [16]?

(3) Are any other polarization dynamical phenomena possible in gas lasers with weakly anisotropic cavities?

The article is arranged as follows: the simplified mathematical model of a single-mode (two-frequency) gas laser with arbitrary states of polarization of emitted waves and with the active medium placed in the axial magnetic field is considered in Sec. II. In Sec. III polarization instability and multistability phenomena are studied theoretically (analytically and numerically) at different anisotropies of the empty cavity and active medium. Section IV describes the experiments on the He-Ne ($\lambda=1.15\ \mu$m) laser with polarization instability in the case of orthogonal elliptically polarized eigenstates of the cavity.

II. MATHEMATICAL MODEL

The equations of motion for a single-longitudinal-mode (two-frequency) standing-wave gas laser with anisotropic cavity were derived on the basis of the Jones vectors and matrices formalism in [16]. The electromagnetic field in such a laser is given as a superposition of four running components with slowly varying with time amplitudes, phases, ellipticities, and azimuths, which form a field of two standing waves with arbitrary in the general case intensities, frequencies, and states of polarization denoted by subscripts 1 and 2. See for details [16]. We consider here a simplified model of a single-mode gas laser with an active medium placed in a longitudinal magnetic field, which follows from [16] in the case where the influence of a magnetic field is taken into account only in the linear part of the equations which is independent of the intensity. This simplification does not restrict the generality of the problem stated in the present work and, nevertheless, it permits simplifying considerably the procedure of calculating the coefficients of nonlinear interaction. The geometry of the anisotropic-cavity gas laser is given in Fig. 1. The temporal evolution of intensities, phases, ellipticities, and azimuths of emitted waves 1 and 2 at the point P of the cavity is described by the system of eight scalar ordinary first-order differential equations which is of the form

$$\frac{dI_1}{d\tau}+2iI_1\frac{d\Psi_1}{d\tau}$$
$$=2I_1\left\{\frac{P_1}{P}+\frac{\Delta W_1}{P}\tanh 2\overline{\xi_1}+i(\omega_1-\omega_{01})\frac{Lc}{\tau_0}-m_1\right.$$
$$+i\tanh 2\overline{\xi_1}\frac{d\Phi_1}{d\tau}+i\frac{\overline{V_1}}{P}-I_1(b_1+d_1\tanh 2\overline{\xi_1^2})$$
$$\left.-I_2\left[a_{12}+b_{12}\frac{\cos 2(\Phi_1-\Phi_2)}{\cosh 2\overline{\xi_1}\cosh 2\overline{\xi_2}}\right.\right.$$
$$\left.\left.+d_{12}\tanh 2\overline{\xi_1}\tanh 2\overline{\xi_2}\right]\right\}, \tag{1}$$

$$\frac{dI_2}{d\tau}+2iI_2\frac{d\Psi_2}{d\tau}$$
$$=2I_2\left\{\frac{P_2}{P}+\frac{\Delta W_2}{P}\tanh 2\overline{\xi_2}+i(\omega_2-\omega_{02})\frac{Lc}{\tau_0}-m_2\right.$$
$$+i\tanh 2\overline{\xi_2}\frac{d\Phi_2}{d\tau}+i\frac{\overline{V_2}}{P}-I_2(b_2+d_2\tanh 2\overline{\xi_2^2})$$
$$\left.-I_1\left[a_{21}+b_{21}\frac{\cos 2(\Phi_2-\Phi_1)}{\cosh 2\overline{\xi_2}\cosh 2\overline{\xi_1}}\right.\right.$$
$$\left.\left.+d_{21}\tanh 2\overline{\xi_2}\tanh 2\overline{\xi_1}\right]\right\}, \tag{2}$$

$$\frac{df_1}{d\tau}=n_1+i\frac{\Delta W_1}{P}-iI_1d_1\tanh 2\overline{\xi_1}+I_2\left[\frac{b_{12}\sin 2(f_1-\Phi_2)}{\cosh 2\overline{\xi_2}}\right.$$
$$\left.-id_{12}\tanh 2\overline{\xi_2}\right], \tag{3}$$

$$\frac{df_2}{d\tau}=n_2+i\frac{\Delta W_2}{P}-iI_2d_2\tanh 2\overline{\xi_2}+I_1\left[\frac{b_{21}\sin 2(f_2-\Phi_1)}{\cosh 2\overline{\xi_1}}\right.$$
$$\left.-id_{21}\tanh 2\overline{\xi_1}\right], \tag{4}$$

$$m_1=\frac{1}{2\tau_0}\left(1-\frac{\lambda_2}{\lambda_1}\right)$$
$$\times\left[\frac{\sin(f_{1M}+f_{2M}-2\Phi_1)+\sin(f_{1M}-f_{2M}-2i\overline{\xi_1})}{\sin(f_{1M}-f_{2M})\cosh 2\overline{\xi_1}}\right], \tag{5}$$

$$n_1=\frac{1}{2\tau_0}\left(1-\frac{\lambda_2}{\lambda_1}\right)\left[\frac{\cos(f_{1M}+f_{2M}-2f_1)}{\sin(f_{1M}-f_{2M})}-\cot(f_{1M}-f_{2M})\right]. \tag{6}$$

Here $I_{1,2}=I'_{1,2}/k_0lP$ is the dimensionless intensity, $\Psi_{1,2}$ is the phase of the emitted wave, $\omega_{1,2}/2\pi$(Hz) and $\omega_{01,02}/2\pi$(Hz) are the lasing and cavity frequencies, respectively; $\Omega=\omega L/(c\tau_0)$, $\tau=\tau_0tL/c$, l and L are the active medium and cavity lengths, respectively; c is the velocity of light, t is the time, $\tau_0=k_0lP$, η is the pump excess over the threshold at the line center, $f_{1,2}=\Phi_{1,2}+i\overline{\xi}_{1,2}$, $\xi_{1,2}=\tanh\overline{\xi}_{1,2}$, Φ is the azimuth, $\xi=\tanh\overline{\xi}$ is the ellipticity of the electromagnetic wave, $I'=|\overline{E}|^2|d_{ab}|^2/3\hbar^2\gamma_a\gamma_b$, $|d_{ab}|$ is the reduced matrix element of the dipole moment of the transition, $\overline{E}$ is the Jones vector of the electromagnetic wave, $\gamma_{a,b}$ are the relaxation constants of the lower and upper working levels, respectively, $k_0=2\pi^{3/2}N|d_{ab}|^2\omega/3\hbar cKu$ is the linear gain coefficient, N is the inversion population density, $W(x\pm\Delta,y)=U(x\pm\Delta,y)+iV(x\pm\Delta,y)$ is the complex error function; $\overline{W}=\overline{U}+i\overline{V}=[W(x-\Delta,y)+W(x+\Delta,y)]/2$, $\Delta W=[W(x-\Delta,y)-W(x+\Delta,y)]/2$, $x\pm\Delta=(\omega-\omega_0\pm g\mu_BH)/Ku$ is the detuning of the laser frequency ω from the line center ω_0, g is the Lande factor, μ_B is the Bohr magneton, H is the magnetic field strength, $y=\gamma/Ku$, 2γ is the homogeneous linewidth, $P_{1,2}=\overline{U}-1/\eta_{1,2}$, $P=\overline{U}|_{x=0}-(1/\eta_1+1/\eta_2)/2$, $Ku=\Delta\omega_D/2(\ln 2)^{1/2}$, $\Delta\omega_D$ is the Doppler linewidth, and $\lambda_{1,2}$ and $f_{1M,2M}$ are the eigenvalues and eigenvectors (eigenstates) of the empty cavity matrix $\hat{M}$, respectively. The expressions for m_2 and n_2 are obtained from m_1 and n_1 by reversing indices 1 and 2. The self-saturation coefficients. $b_1,d_1(b_2,d_2)$ as well as the cross-saturation coefficients a_{12},b_{12},d_{12} (a_{21},b_{21},d_{21}) have been obtained in the Doppler limiting case in the approximation of three relaxation constants. They take on the following forms:

$$b_1=(R_1+R_2+R_3)L_0,\quad d_1=(R_1-R_2-R_3)L_0, \tag{7}$$

$$a_{12}=[(R_1+R_3)y_1+(R_1+R_2)y_2]L_1+[(R_1+R_3)L_3$$
$$+(R_1+R_2)L_4]L_2. \tag{8}$$

The expressions for b_{12} and d_{12} are obtained from a_{12} under the substitutions $R_1+R_3\rightarrow R_2, R_1+R_2\rightarrow R_3$ and $R_1+R_3\rightarrow R_1-R_3, R_1+R_2\rightarrow R_1-R_2$;

$$L_0=\exp(-x_1^2)\frac{y_1+y_2}{y}\left(1+\frac{y}{y+ix_1}\right), \tag{9}$$

$$L_1=\exp(-x_1^2)\left(\frac{1}{y+i\Delta x}+\frac{1}{y+ix}\right), \tag{10}$$

$$L_2=\exp(-x_1^2)y_1y_2\left(\frac{1}{y+i\Delta x}+\frac{N_{12}}{y+ix_1}\right), \tag{11}$$

$$L_3=\frac{1}{y_1+i\Delta x},\quad L_4=\frac{1}{y_2+i\Delta x}. \tag{12}$$

Here $x=(x_1+x_2)/2$, $\Delta x=(x_1-x_2)/2$, $y_{1,2}=\gamma_{a,b}/2Ku$, and R_1,R_2,R_3 are the angular momenta functions [16] (for the $j_b=1\rightarrow j_a=2$ transition $R_1=0.46$, $R_2=0.01$, $R_3=0.21$, for the $j_b=2\rightarrow j_a=2$ transition $R_1=0.26$, $R_2=0.21$, $R_3=0.21$), $N_{12}=N'_{12}/N$ is the ratio of the Fourier component of the inverse population density to its value averaged over the cavity length [24]:

$$N_{12}=\int_0^L N(z)e^{-2i(K_1-K_2)z}dz\Big/\int_0^L N(z)dz. \tag{13}$$

The coefficients $b_2, d_2, a_{21}, b_{21}, d_{21}$ are obtained from $b_1, d_1, a_{12}, b_{12}, d_{12}$ by replacing $x_{1,2}$ with $x_{2,1}$ in expressions (9)–(12).

In spite of the fact that the phases of emitted waves do not influence polarization instability, as shown in [16], these variables are included in the consideration, since they will be used further to explain the experimental results.

III. SPONTANEOUS PULSATIONS AND POLARIZATION MULTISTABILITY AT DIFFERENT CAVITY ANISOTROPIES AND DIFFERENT TRANSITIONS BETWEEN THE WORKING LEVELS (THEORY)

Polarization of radiation in the anisotropic-cavity gas laser is determined by the nonlinear anisotropic properties of the active medium, anisotropy of the empty cavity, and external fields [4]. Therefore it makes sense to see, from the point of view of the model proposed, how each of these factors influences polarization instability.

A. Anisotropic properties of the active medium in a single-mode gas laser

A gas medium which is isotropic in the absence of lasing becomes anisotropic due to the nonlinear interaction with emitted polarized radiation, or due to the influence of external fields. The anisotropic properties of the gas medium irradiated by two elliptically polarized waves were studied in [34]. In the case of isotropic cavity, the state of polarization of the emitted field is fully determined by the active medium anisotropy, which is governed mainly by the type of transition between the working levels.

As is known (see, for example, [30]), in a single-mode isotropic-cavity gas laser at the $j \rightarrow j+1$ transitions ($j>0$) the linearly polarized wave is stable, while at the $j \rightarrow j$ transitions ($j \neq 1/2$) the circularly polarized wave is stable.

We do not consider the neutral transitions $j_b=0 \rightarrow j_a=1, j_b=1/2 \rightarrow j_a=1/2$ in this paper. They can be considered on the basis of Eqs. (1)–(4) with a more complicated model of relaxation constants. Polarization dynamics for the neutral transition $j_b=0 \rightarrow j_a=1$ is investigated in detail in [5,6].

B. Linear phase anisotropy of the cavity

Spontaneous pulsations and multistability in a laser with linear phase anisotropy were studied in detail in earlier works [16] and here we shall briefly recall the principal results.

Anisotropy of such a type arises when a birefringent plate is placed inside the cavity. As shown in [40], amplitude anisotropy leads to the stable one-frequency operation, therefore we shall investigate hereinafter mainly the influence of phase anisotropy on polarization instability.

In the case of equal intensities ($I_1=I_2$) and orthogonal states of polarization ($\Phi_2=\Phi_1+\pi/2$, $\xi_2=-\xi_1$) of emitted waves, when the changes in intensity with time can be neglected ($I_1=I_2=I_0$), Eq. (3) is reduced to

$$\frac{df_1}{d\tau}=-\frac{1}{2\tau_0}(1-e^{4i\psi})\sin 2f_1 - iI_0\theta_2 \tanh 2\overline{\xi_1}, \qquad (14)$$

$$\theta_2 = d_1 - d_{12} + b_{12} = (R_1 - R_2 - R_3)(y_1+y_2)\exp(-x_1^2)(1+N_{12})/y. \qquad (15)$$

At the $j \rightarrow j+1$ transitions ($j>0$) $R_1-R_2-R_3>0$, at the $j \rightarrow j$ transitions ($j \neq 1/2$) $R_1-R_2-R_3<0$, and at the neutral transitions this expression is equal to zero.

Under the assumption that $\Delta x \ll y_{1,2}, y_{1,2}=\gamma_{a,b}/2Ku$; in the vicinity of the line center ($x \ll y$) the stationary solutions to Eq. (14) can be found analytically:

$$\Phi_1=0, \ \pm\pi/2, \xi_1=0, \qquad (16)$$

$$\Phi_1=\pm\pi/4, \ \sinh 2\overline{\xi_1}=\pm\{-\alpha/2q-(\alpha^2/4q^2-1)^{1/2}\}, \qquad (17)$$

$$\Phi_1=\pm\pi/4, \ \sinh 2\overline{\xi_1}=\pm\{-\alpha/2q+(\alpha^2/4q^2-1)^{1/2}\}. \qquad (18)$$

Here $\alpha=2\tau_0\theta_2, q=\sin 4\psi$, 2ψ is the value of linear phase anisotropy.

For the $j \rightarrow j$ transitions at all values of ψ two orthogonal linearly polarized waves, described by Eq. (16), are stable. For the $j \rightarrow j+1$ transitions in the region of ψ: $\alpha/4<\sin 2\psi<(\alpha/4)^{1/2}$, a steady-state regime with periodic oscillations of intensity, ellipticity, and azimuth of the emitted field is realized. The limit cycle occurs at the point $\psi^*=(1/2)\arcsin(\alpha/4)^{1/2}$ due to the Hopf bifurcation and is destroyed at the point $\psi^{**}=(1/2)\arcsin(\alpha/4)$ due to the appearance on it of the steady-state saddle-node point (see, for example, [41]).

The longitudinal magnetic field imposed on the active medium in the presence of linear phase anisotropy of the cavity provides a wide variety of one- and two-frequency regimes considered in [16].

C. Circular phase anisotropy of the cavity

Circular phase anisotropy arises in a standing-wave gas laser with a Faraday element inside the cavity. In the case of equal intensities and orthogonal states of polarization of emitted waves, which is realized in the vicinity of the line center, Eqs. (1)–(4) are reduced to a system of three nonlinear first-order differential equations of the following form:

$$\frac{dI_1}{d\tau}=2I\mathrm{Re}\left\{\frac{P_1}{P}-\frac{1}{2\tau_0}(1-e^{2i\phi})(1-\tanh 2\overline{\xi_1}) - I_1(\theta_1+\theta_2\tanh 2\overline{\xi_1^2})\right\}, \qquad (19)$$

$$\frac{df_1}{d\tau}=\frac{i}{2\tau_0}(1-e^{2i\phi})-iI_1\theta_2\tanh 2\overline{\xi_1}+i\frac{\Delta W}{P}, \qquad (20)$$

2ϕ is the value of circular phase anisotropy.

As follows from Eqs. (19) and (20), the intensity and ellipticity do not depend on the azimuth. Because θ_2 is a real function, at $\Delta x \ll y_{1,2}$, the azimuth, in turn, changes independently of these two variables. In this case, the influence of the longitudinal magnetic field can be easily taken into account. Indeed, at the line center tuning ($x=0$),

$$\Delta W=\Delta W'+i\Delta W''\approx 2\Delta\{\Delta x(1-4y/\sqrt{\pi})+i[y-1/\sqrt{\pi}+2(\Delta^2/3-y^2+\Delta x^2+\Delta xy/\Delta)/\sqrt{\pi}]\}$$

and $\Delta W' \ll \Delta W''$, so that the magnetic field practically influences only the rate of azimuth rotation. It is also obvious that circular phase anisotropy in the cavity (the Faraday laser) and a longitudinal magnetic field on the active medium (the Zeeman laser) at $x=0$ equally influence the state of polarization of the emitted field.

The stationary solutions for intensity and ellipticity can be found analytically:

$$I_1=\frac{(P_1/P-a)}{\theta_1},\quad \tanh 2\overline{\xi_1}=\frac{a\theta_1}{(P_1/P-a)\theta_2}, \tag{21}$$

$$I_1=\frac{P_1/P}{\theta_1+\theta_2},\quad \tanh 2\overline{\xi_1}=+1, \tag{22}$$

$$I_1=\frac{(P_1/P-2a)}{\theta_1+\theta_2},\quad \tanh 2\overline{\xi_1}=-1, \tag{23}$$

$a=(1-\cos 4\phi)/2\tau_0$.

The stability analysis of these solutions shows that for the $j\to j+1$ transitions at all values of the cavity anisotropy ϕ the solution (22) is stable (equilibrium state is the node), the solution (23) exists but it is unstable. For the $j\to j$ transitions in the region of ϕ, satisfying the inequality $\phi<\phi^*=0.5\{\tau_0 P_1\theta_2/[P(\theta_1+\theta_2)]\}^{1/2}$, the solution (21) is unstable. It describes a wave with a rotating azimuth, constant intensity, and ellipticity whose value depends on the value of the cavity anisotropy. At $\phi>\phi^*$ a wave with right circular polarization (22) is realized, the solution (23), describing a wave with left circular polarization, is unstable.

The analytical solutions (16)–(18), (21)–(23) enable us to follow the evolution of the state of polarization of the emitted field when the anisotropy of the empty cavity grows from zero and it changes from isotropic at $\psi=0$ ($\phi=0$) to strongly anisotropic at $\psi>\psi^*$ ($\phi>\phi^*$). At very small $\psi(\phi)\neq 0$ for the $j\to j+1$ transitions one linearly polarized wave breaks down into two orthogonal circularly polarized waves meanwhile for the $j\to j$ transitions one circularly polarized wave breaks down into two orthogonal linearly polarized waves with different frequencies. Instabilities arise when polarization of these two waves and polarization of the cavity eigenstates differ greatly from each other. The empty cavity anisotropy, affecting the emitted field polarization, changes the anisotropy of the active medium, and the atoms of the medium begin to irradiate the electromagnetic field whose polarization is determined mainly by the anisotropy of the cavity. In this case, the scheme of connection between the atomic sublevels is changed. Precisely this fact shows obviously that polarization instability is a manifestation of the competition between the anisotropies of the nonlinear active medium and empty cavity.

D. Elliptical orthogonal eigenstates of the cavity

Elliptical orthogonal eigenstates are realized in the cavity with a birefringent plate 1 and a Faraday element 2 (Fig. 1).

The Jones matrix of the cavity $\hat{M}$ for one round-trip with the above-mentioned sequence of elements when starting at the point P and going in the direction (+) takes on the form

$$\hat{M}=\hat{M}^+\hat{M}^-=\begin{pmatrix}\cos\phi & -\sin\phi\\ \sin\phi & \cos\phi\end{pmatrix}\begin{pmatrix}e^{i\psi} & 0\\ 0 & e^{-i\psi}\end{pmatrix}\begin{pmatrix}e^{i\psi} & 0\\ 0 & e^{-i\psi}\end{pmatrix}\times\begin{pmatrix}\cos\phi & -\sin\phi\\ \sin\phi & \cos\phi\end{pmatrix}$$

$$=\begin{pmatrix}e^{2i\psi}\cos^2\phi-e^{-2i\psi}\sin^2\phi & -\sin 2\phi\cos 2\psi\\ \sin 2\phi\cos 2\psi & e^{-2i\psi}\cos^2\phi-e^{2i\psi}\sin^2\phi\end{pmatrix}. \tag{24}$$

Here ψ and ϕ are the values of linear and circular phase anisotropy, respectively.

This configuration of elements is convenient for controlling polarization of radiation in practice. Creating a small constant linear phase anisotropy and adjusting the value of current in the Faraday element, it is possible to change the eigenstates of the cavity from linear to circular ones. The eigenvalues of the matrix $\hat{M}$ are found analytically:

$$\lambda_{1,2}=\cos 2\psi\cos 2\phi\pm\sqrt{\cos^2 2\psi\cos^2 2\phi-1}, \tag{25}$$

and the frequency difference between the cavity eigenstates is determined by the expression

$$\omega_{01}-\omega_{02}=2\arccos(\cos 2\psi\cos 2\phi)c/L. \tag{26}$$

Polarization of the cavity eigenstates satisfying the conditions [34]

$$\frac{m_{12}+m_{21}}{m_{11}-m_{22}}=-\cot[\Phi_{1M}+\Phi_{2M}+i(\overline{\xi}_{1M}+\overline{\xi}_{2M})],$$

$$\frac{m_{21}-m_{12}}{m_{11}-m_{22}}=-\frac{\cos[\Phi_{1M}+\Phi_{2M}+i(\overline{\xi}_{1M}+\overline{\xi}_{2M})]}{\sin[\Phi_{1M}+\Phi_{2M}+i(\overline{\xi}_{1M}+\overline{\xi}_{2M})]}, \tag{27}$$

where m_{ij} are the elements of the matrix $\hat{M}$, takes on the form

$$\Phi_{1M}=0,\ \sinh 2\overline{\xi}_{1M}=-\sin 2\phi\cot 2\psi,$$

$$\Phi_{2M}=\pi/2,\ \xi_{2M}=-\xi_{1M}. \tag{28}$$

The major axes of ellipses of the cavity eigenstates which are determined by expressions (28) coincide with the principal axes of the birefringent plate. In this case, the equations of motion (1)–(4) near the central tuning are written in the following form:

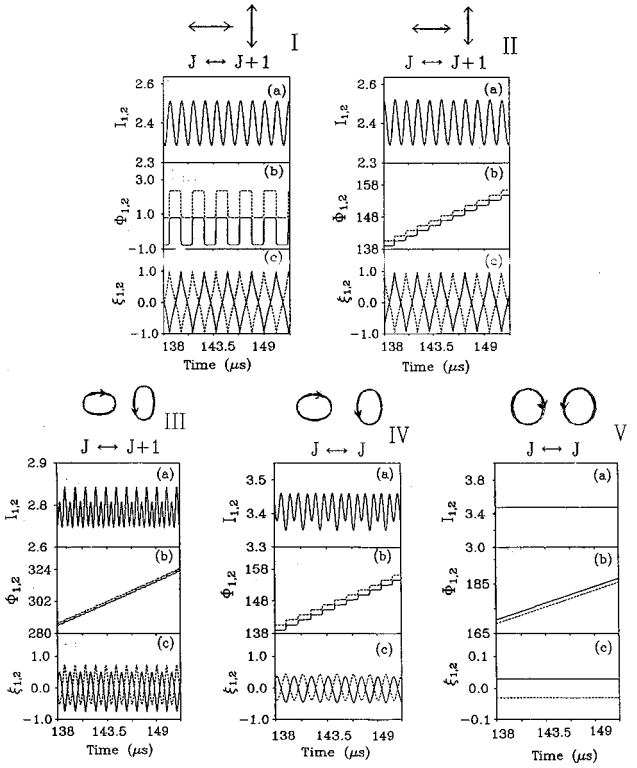

FIG. 2. Polarization instability at different eigenstates of the empty cavity and different transitions between the working levels (shown at top of each column). Temporal evolution of intensities (a), azimuths (rad) (b), and ellipticities (c) has been calculated for $\psi=1$ mrad, $H=0$ (I), $\psi=1$ mrad, $H=1$ Oe (II), $\psi=1$ mrad, $\phi=0.25$ mrad, $H=0$ (III), $\psi=1$ mrad, $\phi=1$ mrad, $H=0$ (IV), and $\phi=1$ mrad, $H=0$ (V).

$$\frac{dI_1}{d\tau}=2I_1\mathrm{Re}\left\{\frac{P_1}{P}-\frac{1}{2\tau_0}\left(1-\frac{\lambda_2}{\lambda_1}\right)\left(1-\frac{\cos 2\Phi_1}{\cosh 2\overline{\xi}_{1M}\cosh 2\overline{\xi}_1}-\tanh 2\overline{\xi}_{1M}\tanh 2\overline{\xi}_1\right)-I(\theta_1+\theta_2\tanh 2\overline{\xi^2})\right\}, \quad (29)$$

$$\frac{df_1}{d\tau}=\frac{1}{2\tau_0}\left(1-\frac{\lambda_2}{\lambda_1}\right)\left(\frac{-\sin 2f_1}{\cosh 2\overline{\xi}_{1M}}+i\tanh 2\overline{\xi}_{1M}\right)-iI_1\theta_2\tanh 2\overline{\xi}. \quad (30)$$

At $\xi_{1M,2M}=0$ (birefringence only) and at $\xi_{1M,2M}=\pm 1$ (Faraday rotation only) the equations of motion for orthogonal linearly and circularly polarized eigenstates of the empty cavity follow from Eqs. (29) and (30).

Figure 2 illustrates spontaneous pulsations at different transitions between the working levels and different eigenstates of the empty cavity, whose polarization changes from a linear (column *I*) to a circular (column *V*) one (shown at top of each column). Here the results are presented of the numerical integration of Eqs. (1)–(4) at the following parameters of the active medium and empty cavity of the He-Ne laser ($\lambda=0.63$ μm), $\eta_1=\eta_2=1.9$, $c/L=612$ MHz, $y_1=0.011$, $y_2=0.005$, $y=0.2$, $k_0 l=0.025$, $x=0$, $Ku=870$ MHz. The initial conditions are taken as follows: $I_1^0=I_2^0=\xi_1^0=\xi_2^0=0$, $\Phi_1^0=0$, $\Phi_2^0=\pi/2$.

Spontaneous pulsations of intensities (a), azimuths (b), and ellipticities (c) of the waves 1 and 2, shown by solid and dashed lines, are given in Fig. 2, I at $\psi=1$ mrad, $\phi=0$, $H=0$ Oe and Fig. 2, II at $\psi=1$ mrad, $\phi=0$, $H=1$ Oe for the $j_b=1\rightarrow j_a=2$ transition without and with the Earth magnetic field, respectively. Figure 2, III and Fig. 2, IV show spontaneous pulsations in the case of orthogonal elliptically polarized eigenstates of the cavity for small ($\psi=1$ mrad, $\phi=0.25$ mrad, $H=0$) and large ($\psi=1$ mrad, $\phi=1$ mrad, $H=0$) values of ellipticity, at the $j_b=1\rightarrow j_a=2$ and $j_b=2\rightarrow j_a=2$ transitions, respectively. Figure 2, V shows polarization instability, which appears as rotation of azimuths with constant intensities and ellipticities, at circularly polarized eigenstates of the cavity and $j_b=2\rightarrow j_a=2$ transition for ($\psi=0$ mrad, $\phi=1$ mrad, $H=0$). Hereinafter all the parameters, except for the coefficients R_1, R_2, R_3, are the same for the $j\rightarrow j+1$ and $j\rightarrow j$ transitions.

It follows from the results presented in Fig. 2 that spontaneous pulsations in a single-mode gas laser with weakly anisotropic cavity exist at both the $j\rightarrow j+1$ and $j\rightarrow j$ transitions for small (including zero) and large values of ellipticities of the cavity eigenstates, respectively. They manifest themselves as periodic oscillations of intensities, ellipticities, and azimuths of two emitted waves or as oscillations of intensities and ellipticities and rotation of azimuths. Such a behavior corresponds to the limit cycles of the first or the second kind.

The influence of the frequency detuning from the gain profile center on the operation of the single-longitudinal-mode laser has been studied in the region of phase anisotropy values where polarization instability takes place. It has been found that besides spontaneous pulsations, one-frequency stationary regimes with orthogonal states of polarization given by the cavity are possible, and the laser operation depends on the initial states of polarization, i.e., polarization multistability takes place.

Figure 3 illustrates polarization multistability at different eigenstates of the empty cavity and different transitions between the working levels. The parameters of the active medium and empty cavity are the same as in Fig. 2. Polarization multistability in the case of linear phase anisotropy of the cavity is shown in Fig. 3, I, II under several different initial conditions: $I_{1,2}^0=\Phi_1^0=\xi_{1,2}^0=0, \Phi_2^0=\pi/2$ (a), $I_{1,2}^0=0, \xi_{1,2}^0=\pm 1$ (b), $I_{1,2}^0=\xi_{1,2}^0=\Phi_{1,2}^0=0$ (c), $I_{1,2}^0=\xi_{1,2}^0=0, \Phi_{1,2}^0=\pi/2$ [(d), I], $I_{1,2}^0=0, \xi_{1,2}^0=1$ [(d), II]. Here solid and dashed lines denote the emitted wave 1 with ($\Phi_1=0, \xi_1=0$) and wave 2 with ($\Phi_2=\pi/2, \xi_2=0$), respectively; the triangular-marked line hereinafter shows spontaneous pulsations. The arrows in Fig. 3 indicate the transition between two stationary orthogonally polarized solutions at large detunings which occurs through a very narrow region with polarization instability. Figure 3 II shows the same as Fig. 3 I, but in the presence of a small Earth magnetic field, which widens the region of detunings where spontaneous pulsations take place. The transition between two orthogonal linearly polarized waves which occurs through the region of detunings with polarization instability, shown in Fig. 3, I(a) and Fig. 3, II(a), was observed experimentally in the He-Ne laser ($\lambda=3.3922$ μm, $j_b=1\rightarrow j_a=2$

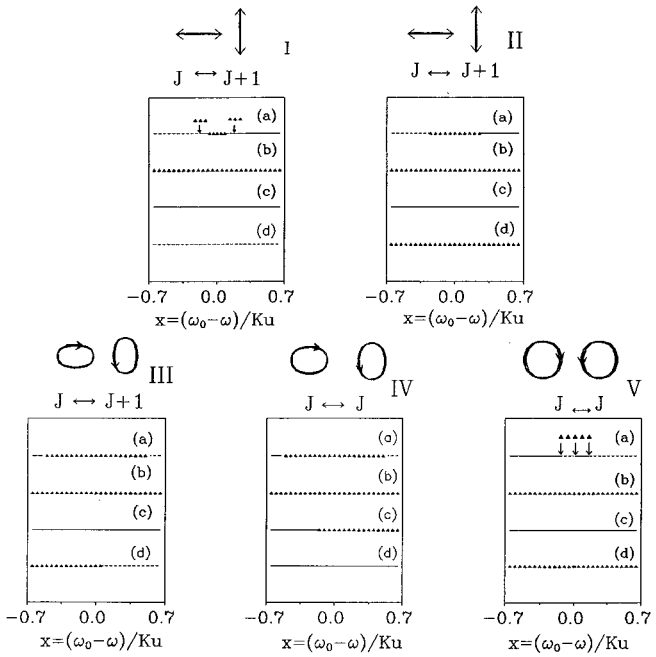

FIG. 3. The schematical representation of polarization multistability at different eigenstates of the empty cavity and different transitions between the working levels. All the parameters are the same as in Fig. 2.

transition) with linear phase anisotropy of the cavity in [9]. Polarization multistability in the case of elliptically polarized eigenstates of the cavity is shown in (Fig. 3, III, IV). The initial conditions in column III are $I^0_{1,2}=\Phi^0_1=0$, $\xi^0_{1,2}=\pm 0.24, \Phi^0_2=\pi/2$(*a*), $I^0_{1,2}=0, \xi^0_{1,2}=\pm 1$ (b), $I^0_{1,2}=\Phi^0_{1,2}=\xi^0_{1,2}=0$ (c), $I^0_{1,2}=0, \xi^0_{1,2}=1$ (d); in column IV $I^0_{1,2}=\Phi^0_1=0$, $\xi^0_{1,2}=\pm 0.4, \Phi_2=\pi/2$ (a), $I^0_{1,2}=\Phi^0_1=\xi^0_{1,2}=0, \Phi^0_2=\pi/2$ (b), $I^0_{1,2}=\Phi^0_{1,2}=\xi^0_{1,2}=0$ (c), $I^0_{1,2}=0, \xi^0_{1,2}=1$ (d). Here solid and dashed lines represent the stationary states of polarization, determined by the empty cavity. Polarization multistability in the case of circular phase anisotropy of the cavity is represented schematically in Fig. 3, V for the initial conditions $I^0_{1,2}=\Phi^0_1=\xi^0_{1,2}=\pm 1$ (a), $I^0_{1,2}=\Phi^0_1=\xi^0_{1,2}=0, \Phi^0_2=\pi/2$ (b), $I^0_{1,2}=0, \xi^0_{1,2}=1$ (c), $I^0_{1,2}=\xi^0_{1,2}=0, \Phi^0_{1,2}=0$ (d).

Here the solid and dashed lines show the waves with right and left circular polarization, respectively. In the case of orthogonal circularly polarized at the initial moment waves three solutions can be found, and the transition from the right circularly polarized wave to the left circularly polarized wave occurs through the region of detunings with polarization instability [Fig. 3 V(a)]. The polarization behavior of such a type has been observed experimentally in the He-Ne laser ($\lambda=3.3912\ \mu$m, $j_b=1\rightarrow j_a=1$ transition) [11].

Polarization multistability is a consequence of spontaneous pulsations. Depending on the initial states of polarization of emitted waves, it leads to the existence of stationary and self-oscillating regimes in different regions of detunings. This effect can be used in practice to stabilize the operation of lasers with internal mirrors where polarization instability arises due to imperfections of the optical elements.

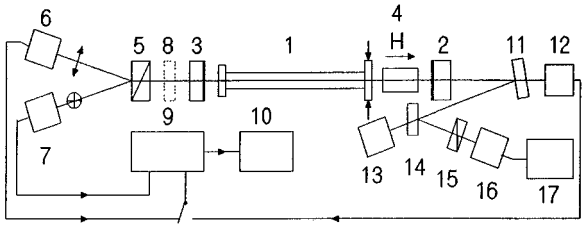

FIG. 4. The schematical representation of the experimental setup.

IV. EXPERIMENTAL STUDIES OF POLARIZATION INSTABILITY AT ELLIPTICAL ORTHOGONAL EIGENSTATES OF THE CAVITY

This section describes the experimental study of the phenomenon of polarization instability with the aim to show the scope of validity of the proposed model.

A. Experimental setup and results

Experimental studies were made using a helium-neon laser operating at the $2S_2$-$2P_4$ ($\lambda=1.15\ \mu$m) transition with adjusted values of circular and linear anisotropy of the cavity, which is schematically represented in Fig. 4. To reduce the influence of vibrations and temperature changes on the emitted radiation parameters, the laser was mounted on a massive plate made of a material having a low coefficient of thermal expansion ($\sim 10^{-7}\ \mathrm{K}^{-1}$) installed on a foundation with vibration isolation. The active element—a gas-discharge tube 1 with the capillary diameter 1.5 mm and active gap length 155 mm was sealed by windows with a high-quality antireflection coating which were tilted to the capillary axis at an angle of $\sim 5°$ in two mutually orthogonal directions. This minimized the residual interference in the windows without affecting the high degree of active element anisotropy as a whole. The 0.36 m long laser cavity is formed by a dielectric flat mirror 2 and mirror 3 with the curvature radius 2.5 m which have reflection coefficients of 99.2%. The Faraday element 4 with antireflection coatings was placed inside the cavity. Circular anisotropy of the cavity was controlled by varying current in the Faraday element. Linear phase anisotropy was adjusted due to the effect of photoelasticity by squeezing one of the active element windows with the aid of a specially designed device with electric current control. The portion of the laser emission that passed through the mirror 3 was divided by the Wollaston prism 5 into horizontally and vertically polarized components which were detected by wideband photodetectors 6 and 7, respectively. Likewise [10] we can also represent the emitted field in a basis set of right and left circular polarizations by inserting a quarter-wave plate ($\lambda/4$) 8 in front of the Wollaston prism, whose principal axes were aligned at $\pi/4$ with respect to those of the Wollaston prism (previously aligned with the plane of the experimental set). The signals from the photodetectors 6 and 7 reached the two-channel digital oscilloscope connected with the aid of an interface to a personal computer 10. The second portion of the emission having passed through the beamsplitting plate 11 reached the photodetector 12 which monitored the total intensity output of

the laser. To check the value of cavity detuning and the mode composition of radiation and to estimate the degree of ellipticity of the emitted field in the single-mode regime, a confocal scanning interferometer 13 was used. The portion of radiation reflected by the beam splitter 14 on passing through the polarizer 15 hit the photodetector 16 which indicated the beat signal in the two-frequency operation. The beat signal's spectrum was controlled by a spectrum analyzer 17.

Since practically all elements in the cavity (mirrors, active element windows, and the Faraday element) feature linear phase anisotropy due to the internal mechanical stresses and the microstructure of the reflecting and antireflecting coatings, preliminary orientation of the active element and the Faraday element with respect to the plane of the set was carried out, so that one of the principal axes of the total phase anisotropy coincided with this plane. Then one of the windows of the gas-discharge tube was squeezed in the direction perpendicular to the set plane, thus creating initial anisotropy of the cavity $\sim 15-20$ mrad. The value of this anisotropy was measured from the beat frequency of orthogonally polarized waves in the two-frequency operation which was provided by imposing a transverse magnetic field on the active medium. Compensation of the initial anisotropy was provided by squeezing the other window of the active element in the orthogonal direction by means of a current-controlled device. Minimization of the total linear phase anisotropy was carried out by the minimum beat signal frequency in the regime of lasing of two stationary elliptically polarized waves. Calibration of the Faraday element was carried out by the beat frequency of circularly polarized waves at central tuning of the cavity and with $\psi \sim 0$. To minimize the influence of the frequency pulling near the region of locking, calibration was carried out at considerable frequency splittings (0.5–2 MHz).

Primary consideration was given to the operation at minimum values of linear phase anisotropy and small values (<5 mrad) of circular phase anisotropy ϕ. At $\phi=0$ in the entire region of detunings a one-frequency regime corresponding to the locking of frequencies was observed. Introduction of circular phase anisotropy inside the cavity leads to a stable two-frequency regime with orthogonal elliptically polarized waves. This regime occurs due to the reduction of the locking zone with increasing ellipticity. The transition from the two-frequency regime to the single-frequency one depends to a great extent on the values of residual phase anisotropy and cavity detuning.

In the linear basis of registration, at the line center tuning when circular phase anisotropy ϕ decreases from the values corresponding to the sinusoidal form of the indicated signal [Fig. 5(a)] to zero, there occurs first a distortion of the sinusoidal shape of the beat signal [Fig. 5(b)]. In a very narrow range of ϕ values between the region of two-frequency operation and the locking zone, antiphase periodic changes in the orthogonally polarized components having the form of spikes take place [Fig. 5(c)]. Figure 5 shows the temporal evolution of the xy components I_x, I_y and the total intensity I of the signal from sinusoids to spikes at $\phi=1$ mrad (a), $\phi=0.6$ mrad (b), $\phi=0.4$ mrad (c). The intensities $I_{1,2}$, ellipticities $\xi_{1,2}$, and azimuths $\Phi_{1,2}$ were calculated at $\psi=1$ mrad, $\phi=1$ mrad (a); $\psi=0.8$ mrad, $\phi=0.5$ mrad (b); $\psi=0.6$ mrad, $\phi=0.3$ mrad (c). The idea of the experiment is illustrated by the diagram in Fig. 6, which shows the steady-state solutions to Eqs. (29) and (30) on the plane of ψ and ϕ calculated numerically at central tuning for the experimentally explored parameters. Region I, where the limit cycle of the second kind exists, is bounded by the line on which the Hopf supercritical bifurcation takes place. On the ψ axis the limit cycle of the first kind is realized, in region II two orthogonal elliptically polarized waves appear. The path in the experiment from stationary to nonstationary two-frequency operation [from (a) to (c) in Fig. 5] is shown by an arrow.

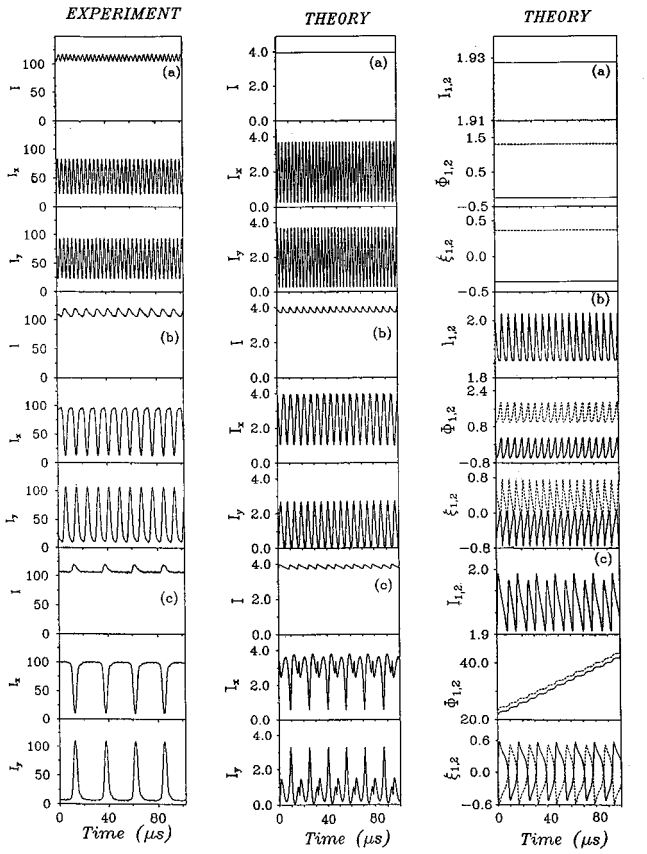

FIG. 5. Temporal evolution of the xy components' intensities $I_{x,y}$ and the total intensity I from sinusoids, observed at $\phi=1.1$ mrad (a) through the distorted sinusoids, observed at $\phi=0.56$ mrad (b) to spikes, observed at $\phi=0.49$ mrad (c). The numerical simulation was carried out, respectively, at $\psi=0.9$ (a), 0.75 (b), and 0.56 mrad (c); $\phi=1.1$ (a), 0.45 (b), and 0.23 mrad (c). The experimental values of $I_{x,y}, I$ hereinafter are given in arbitrary units.

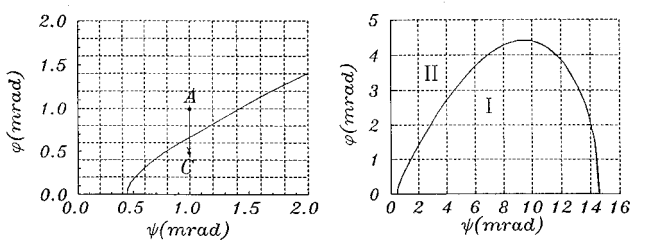

FIG. 6. The diagram of attractors on the plane of linear and circular phase anisotropy parameters calculated at central tuning $x=0$.

Here sinusoids appear at point A, distorted sinusoids are located near the line of the Hopf bifurcation, and large spikes were found at point C. The spike repetition period changes slowly with the drift of the cavity parameters and it is very sensitive to changes in ψ, ϕ, and cavity detuning. In spite of the significant changes in orthogonal components, the total intensity of two waves was modulated at $\leqslant(10-15)\%$ of the cw level and it has the same frequency of oscillations as orthogonally polarized components. Such features have been found both for the distorted sinusoidal signals and for spikes.

The oscillations of the total intensity have been observed in the case of linear phase anisotropy of the cavity in [9,10]. In the case of circular phase anisotropy of the cavity the total intensity was constant [11]. All the experimental observations are in agreement with theory (see Fig. 2).

The transition from the two- to one-frequency regime is asymmetric about the detuning. For instance, in scanning the cavity length from the region of negative values of x through the center, first the one-frequency operation of an elliptically polarized wave with $\xi\sim 0.3$ is observed, then the region of polarization instability with spikes in the orthogonally polarized components appears. Next comes the region with antiphase changes in intensities of orthogonal components, which have the shape of distorted sinusoids. Minimum distortion of sinusoidal signal takes place at central tuning. At a given value of detuning $x>0$ there occurs a transition to the region of one-frequency operation of an elliptically polarized wave whose ellipse major axis is perpendicular to the ellipse major axis of the wave observable at $x<0$. The transition between two stationary orthogonal elliptically polarized waves is illustrated by Fig. 3, III(a). Analogous behavior of polarization parameters has been observed experimentally in [9,11] at linear and circular eigenstates of the cavity. Due to the asymmetry of the gain profile the transition to the one-wave stationary operation depending on the value of ϕ, can proceed through the region of spikes or through the region of distorted sinusoids. In the second case, the transition to the locking zone is the same as in the case of the stationary two-wave operation.

Detuning to the range of positive x was accompanied by the switch of orthogonal components which occurs at some positive value of $x\neq 0$. Figure 7 shows the same characteristics as Fig. 6, but at $x=0.145$(75 MHz).

The polarization behavior for the negative detunings is very much the same as for the positive ones, but the intensities of waves 1 and 2, as well as the orthogonal components of the registered signal, are replaced.

The registration of a signal in the circular basis has revealed the same conformities as in the linear basis (Fig. 8).

B. Analysis of the experimental results

In experiment, polarization instability manifests itself as periodic oscillations of orthogonal components of the laser output of two qualitatively different forms: distorted sinusoids and large spikes. Distorted sinusoids appear near the Hopf bifurcation point. The spikelike oscillations were observed in the narrow region of parameters on going from the two-frequency operation to the locking zone: at the line center tuning when the frequency difference of emitted waves is decreased and at detuning from the line center. Theoretically, polarization instability has been found at the same values of

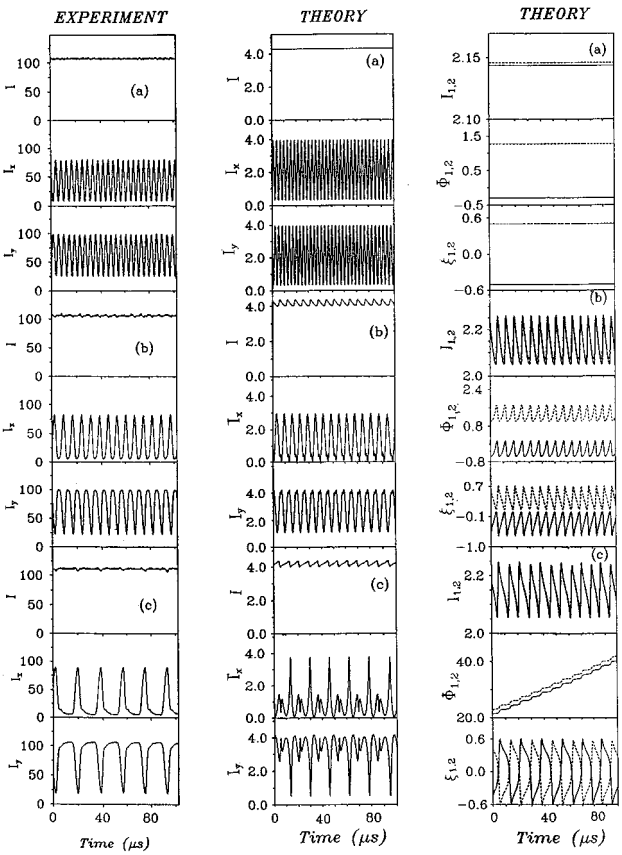

FIG. 7. Same as in Fig. 5, but at the detuning from the line center ($x=0.15$).

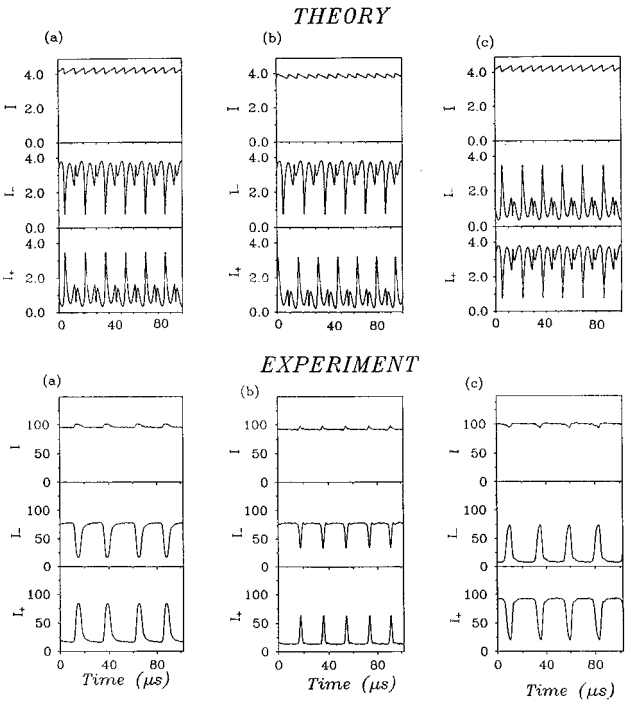

FIG. 8. The spikelike $\pm$ orthogonal components of the laser output, observed experimentally in the circular basis and calculated numerically at $x=-0.15$ (a), $x=0$ (b), and $x=0.15$ (c).

parameters (see Fig. 6 and theoretical curves in Figs. 5, 7, 8), and it appears as spontaneous pulsations of the characteristics of two emitted waves (laser eigenstates). To compare these two manifestations of the phenomenon, let us consider the experimentally registered signal, which represents the interference of coinciding components of two nonstationary laser eigenstates observed in the orthogonal linear and circular bases.

It should be noted that the laser radiation in the self-pulsing regime is neither monochromatic nor completely polarized. Nevertheless it can be described by the Jones vector whose amplitude and phase slowly vary with time, but the frequency is constant and equal to the mean frequency of the wave package Ω, which is the lasing frequency in Eqs. (1) and (2) [$\Omega=\omega L/(c\tau_0)$]. In the xy basis, this vector takes on the form [42,34]

$$\vec{E}=\left(\frac{I(\tau)}{\cosh 2\overline{\xi}(\tau)}\right)^{1/2}\begin{pmatrix}\cos f(\tau)\\ \sin f(\tau)\end{pmatrix}\exp\{i[\Psi(\tau)+\widetilde{\Psi}]\}. \tag{31}$$

Here $\Psi(\tau)$ is the phase slowly varying with time which, according to [42], is determined as $\Psi(\tau)=\Psi_x(\tau)+\Psi'_x(\tau)$ and is the solution to Eqs. (1) and (2), $\Psi_x=\arctan(\xi\tan\Phi)$, $\widetilde{\Psi}=-\Omega\tau-Kz+\Psi(0)$, $\Psi(0)$ is the phase at the initial moment $\tau=0$, and Kz is the optical path length along the cavity axis. The lasing frequency in the nonstationary regime Ω can be regarded as the ''reference-frame frequency'' (see, for example, [43,44]). In the slowly varying amplitude approximation for times smaller than the inverse value of the spectral linewidth and much larger than the period of oscillations at the optical frequency, the radiation, described by expression (31), can be considered as monochromatic and completely polarized [42]. Let us consider the interference of the coinciding components of such two waves. In the xy basis, the intensities I_x and I_y of the components e and c of the registered signal are determined as

$$I_x=|E_{x1}+E_{x2}|^2=|E_{x1}|^2+|E_{x2}|^2+\widetilde{I}_x,$$

$$\widetilde{I}_x=2\,\mathrm{Re}\{E_{x1}E^*_{x2}\exp[i(\Delta\Psi_s+\Delta\Psi_0)]\}, \tag{32}$$

$$I_y=|E_{y1}+E_{y2}|^2=|E_{y1}|^2+|E_{y2}|^2+\widetilde{I}_y,$$

$$\widetilde{I}_y=2\,\mathrm{Re}\{E_{y1}E^*_{y2}\exp[i(\Delta\Psi_s+\Delta\Psi_0)]\}. \tag{33}$$

Here $\Delta\Psi_s=\Delta\Omega_s\tau=(\Omega_1-\Omega_2)\tau$ is the phase difference caused by the difference of the lasing frequencies of waves 1 and 2, $\Delta\Psi_0=\Psi_1(0)-\Psi_2(0)$ is the initial phase difference. The orthogonality of waves 1 and 2 and the equality of their intensities, which is exact at the center tuning, leads to the equality $E_{x2}=-E^*_{y1}$, $E_{y2}=E^*_{x1}$. Therefore $|E_{x1}|^2+|E_{x2}|^2=|E_{y1}|^2+|E_{y2}|^2$, and the information about the registered signal is contained in the quantities $\widetilde{I}_x,\widetilde{I}_y$. Due to the orthogonality of waves 1 and 2, $E_{x1}E^*_{x2}=-E_{y1}E^*_{y2}$ and $\widetilde{I}_x=-\widetilde{I}_y$. This condition explains the antiphase nature of oscillations of x and y components of the registered signal. The expression for $\widetilde{I}_x$ can be given as

$$\widetilde{I}_x=2E_{0x1}E_{0x2}\cos(\Delta\Psi_x+\Delta\Psi_s+\Delta\Psi_0). \tag{34}$$

This expression contains the following variables, which periodically change with time: the amplitudes of the x components E_{0x1}, E_{0x2}, the phase difference $\Delta\Psi_x$ caused by the complex nature of the electromagnetic wave vector due to the account of polarization parameters, and the phase difference $\Delta\Psi_s$ caused by the difference of the stationary lasing frequencies of waves 1 and 2. It has been found numerically that changes in the amplitudes of xy components are negligible and the main contribution to the registered signal is made by the quantity $\Delta\Psi_x$, which oscillates with the frequency of spontaneous pulsations, and by the quantity $\Delta\Psi_s$, which changes with time with the frequency equal to the stationary frequency difference $\Delta\Omega_s$.

The periodic nature (distorted sinusoids and large spikes) of the registered signal follows from expression (33) in the case where the lasing frequency difference $\Delta\Omega_s$ is equal to the frequency of spontaneous pulsations Ω_{sp}:

$$\Delta\Omega_s=\Omega_{\mathrm{sp}}. \tag{35}$$

We have estimated numerically the lasing frequency difference $\Omega_1-\Omega_2$ at stationary operation when the time derivatives in Eqs. (1)–(4) are equal to zero. This quantity does not satisfy equality (35), the discrepancy is about a few dozens percent. It is known (see, for example, [45]) that the presence of spontaneous pulsations can lead to the appearance of an additional beat frequency. Since the change of the sign of the frequency difference cannot be revealed experimentally, we consider the mean of the absolute value of this quantity: $|\Delta\Omega_s|=|\overline{d\Psi_1/d\tau-d\Psi_2/d\tau}+\Omega_1-\Omega_2|$, where $d\Psi_1/d\tau-d\Psi_2/d\tau$ is the instantaneous frequency difference time averaged over a period of spontaneous pulsations [45].

The instantaneous frequency is determined by the expression

$$\frac{d\Psi_1}{d\tau}=\mathrm{Im}\left\{i\tanh 2\overline{\xi}_1\frac{d\Phi_1}{d\tau}+\frac{\Delta W_1}{P}\tanh 2\overline{\xi}_1+i\frac{\overline{V_1}}{P}i(\Omega_1-\Omega_{01})\right.$$
$$-\frac{1}{2\tau_0}\left(1-\frac{\lambda_2}{\lambda_1}\right)\left(1-\frac{\cos 2\Phi_1}{\cosh 2\overline{\xi}_{1M}\cosh 2\overline{\xi}_1}\right.$$
$$\left.-\tanh 2\overline{\xi}_{1M}\tanh 2\overline{\xi}_1\right)-I_1(b_1+d_1\tanh 2\overline{\xi}_1^2)-I_2\left[a_{12}\right.$$
$$\left.\left.+b_{12}\frac{\cos 2(\Phi_1-\Phi_2)}{\cosh 2\overline{\xi}_1\cosh 2\overline{\xi}_2}+d_{12}\tanh 2\overline{\xi}_1\tanh 2\overline{\xi}_2\right]\right\}. \tag{36}$$

Here Ω_1 is the lasing frequency at stationary operation. The expression for $d\Psi_2/d\tau$ can be obtained from Eq. (36) by replacing index 1 with 2. This value was estimated numerically and it is very close to the frequency of spontaneous pulsations Ω_{sp} (the discrepancy is about a few percent).

A detailed study of the phase characteristics of Eqs. (1) and (2) and different reference-frame frequencies will be carried out in the future.

On going from the linear to the circular basis the radiation is passed through the quarter-wave plate ($\lambda/4$) and the Jones vector components are transformed in the following way:

$$\begin{pmatrix} 1 & 1 \\ -1 & 1 \end{pmatrix}\begin{pmatrix} 1+i & 0 \\ 0 & 1-i \end{pmatrix}\begin{pmatrix} 1 & -1 \\ 1 & 1 \end{pmatrix}\begin{pmatrix} E_x \\ E_y \end{pmatrix}\exp[i\tilde{\Psi}]$$

$$=\frac{\sqrt{2}}{2}\begin{pmatrix} E_x - iE_y \\ -i(E_x + iE_y) \end{pmatrix}\exp[i(\tilde{\Psi}+\Psi_{\mathrm{op}})]$$

$$=\frac{\sqrt{2}}{2}\left(\frac{I}{\cosh 2\overline{\xi}}\right)^{1/2}\begin{pmatrix} \exp[-i\Phi+\overline{\xi}] \\ -i\,\exp[i\Phi-\overline{\xi}] \end{pmatrix}$$

$$\times\exp[i(\tilde{\Psi}+\Psi_{\mathrm{op}})]. \tag{37}$$

The additional phase multiplier Ψ_{op} in Eq. (37) appears due to the change in the optical path length on passing through the plate. This value is the same for both orthogonal components and it is determined as follows [42]:

$$\Psi_{\mathrm{op}}=\exp\{i\arg[(E_x-iE_y)/E_x)]\}.$$

The transition to the circular basis is accompanied by the appearance of an additional phase difference $\Delta\Psi_{\mathrm{op}}=\Psi_{1\mathrm{op}}-\Psi_{2\mathrm{op}}$ of waves 1 and 2 due to the difference of the optical path lengths in the plate caused by the difference of the states of polarization of these waves. Taking into account these facts, we have calculated the output characteristics in terms of circularly polarized components (Fig. 8).

To elucidate the influence of small residual linear amplitude anisotropy $\sim|\lambda_1/\lambda_2|=0.9995$, whose principal axes coincide with principal axes of linear phase anisotropy, on the polarization behavior in the laser under consideration, we have also integrated numerically Eqs. (1)–(4). It has been found that this factor leads to asymmetry about the detuning, observed experimentally on going from spikes to the one-frequency stationary regime with elliptical orthogonally polarized wave on the right and on the left of the line center. Polarization switches between the orthogonal components of nonstationary laser output in the vicinity of the line center occurs also in the presence of small linear amplitude anisotropy. This effect is accompanied by the change of the phase difference of the two emitted waves on π.

Thus the consideration carried out in this section has shown the adequacy of the model of the two-frequency gas laser [16], which confirmed the existence of spontaneous pulsations in the experimentally explored region of parameters and explained all of the polarization effects observed experimentally, including periodical oscillations in the form of distorted sinusoids and large spikes obtained in the linear and circular bases. These oscillations result from the interference of the coinciding components of two nonstationary laser eigenstates in the case where the difference of lasing frequencies of these eigenstates is equal to the frequency of spontaneous pulsations.

V. CONCLUSIONS

We have examined a mathematical model of a two-frequency gas laser, developed on the basis of the matrix approach, on the possibility of existence of spontaneous pulsations and polarization multistability at different cavity anisotropies and different transitions between the working levels with and without an axial magnetic field applied to the active medium. These phenomena have been found at linearly and circularly polarized eigenstates of the empty cavity, which were investigated experimentally in previous works, and predicted at elliptically polarized eigenstates.

In accordance with the theoretical prediction, a series of polarization dynamical phenomena have been observed experimentally in the He-Ne ($\lambda=1.15\ \mu$m) laser at elliptical orthogonally polarized eigenstates of the cavity.

In the case of elliptically polarized eigenstates of the cavity we have revealed experimentally all the known features of the nonstationary behavior of polarization parameters, such as periodic oscillations of two qualitatively different forms (distorted sinusoids and large spikes), the transition between two stationary orthogonally polarized waves in the vicinity of the line center tuning which occurs through the region with polarization instability, and explained them from the point of view of the model proposed. Some of these features were observed in previous works at linearly and circularly polarized eigenstates of the empty cavity. An additional phenomenon has been found: switches between the orthogonally polarized components when the output is nonstationary. The results of the theoretical modeling are in quantitative agreement with the experimental results.

It is shown that the whole diversity of nonstationary polarization phenomena in gas lasers with weakly anisotropic cavities, including polarization multistability, occurs due to spontaneous pulsations of intensities, ellipticities, and azimuths of two emitted waves which appear when the steady states of polarization parameters of these waves become unstable. The experimentally observed periodic oscillations of the orthogonal components of laser output in the form of distorted sinusoids and large spikes are due to the fact that experimentally the interference of two nonstationary eigenstates with a frequency difference equal to the frequency of spontaneous pulsations is registered.

We have proved the existence of spontaneous pulsations in a two-frequency standing-wave gas class-A laser, caused by the competition of empty cavity and active medium anisotropies. Up to now self-oscillating regimes have been known to be only due to the backscattering phenomenon in ring gas class-A lasers.

ACKNOWLEDGMENTS

We are grateful to N.B. Abraham for the fruitful comments and for sharing the results of [5–7] with us before their publication. The research described in this publication was made possible in part by Grant No. RWVOOO from the International Science Foundation.

[1] W. Culshaw, J. Kannelaud, and F. Lopez, Phys. Rev. **128**, 1747 (1962).
[2] W. Culshaw and J. Kannelaud, Phys. Rev. A **141**, 228 (1966); **141**, 237 (1966).
[3] R. Paanen, C. L. Tang, and H. Statz, Proc. IEEE **51**, 61 (1963).
[4] H. de Lang, Philips Res. Rep. Suppl. **8**, 3 (1967).
[5] N. B. Abraham, E. Arimondo, and M. San Miguel, Opt. Commun. **117**, 344 (1995).
[6] N. B. Abraham, M. Matlin, and R. S. Gioggia, Phys. Rev. A **53**, 3514 (1996).
[7] M. D. Matlin, R. S. Gioggia, N. B. Abraham, P. Glorieux, and T. Crawford, Opt. Commun. **120**, 204 (1995).
[8] A. G. May, P. Paddon, J. Sjerve, and G. Stephan, Phys. Rev. A **53**, 2829 (1996).
[9] A. Le Floch, G. Ropars, and J. Lenormand, Phys. Rev. Lett. **52**, 918 (1984).
[10] G. P. Puccioni, G. L. Lippi, N. B. Abraham, and F. T. Arecchi, Opt. Commun. **72**, 361 (1989).
[11] J. C. Cotteverte, F. B. Bretenaker, and A. Le Floch, Opt. Lett. **16**, 572 (1991).
[12] J. C. Cotteverte, F. B. Bretenaker, and A. Le Floch, Opt. Commun. **79**, 321 (1990).
[13] F. B. Bretenaker and A. Le Floch, Opt. Commun. **79**, 314 (1990).
[14] A. D. May and G. Stephan, J. Opt. Soc. Am. B **6**, 2355 (1989); W. Xiong, P. Glanzing, P. Paddon, A. D. May, M. Bourouis, S. Laniepce, and G. Stephan, *ibid.* **8**, 1236 (1991); P. Paddon, E. Sjerve, A. D. May, M. Bourouis, S. Laniepce, and G. Stephan, *ibid.* **9**, 574 (1992).
[15] L. P. Svirina and V. N. Severikov, Opt. Spektrosk. **64**, 208 (1988) [Opt. Spectrosc. **64**, 124 (1988)]; A. P. Voitovich, L. P. Svirina, and V. N. Severikov, Kvant. Elektron. (Moscow) **16**, 912 (1989) [Sov. J. Quantum Electron. **19**, 592 (1989)]; Izv. Akad. Nauk SSSR, Ser. Fiz. **53**, 1131 (1989) [Bull. Acad. Sci. USSR, Phys. Ser. **53**, 102 (1989)]; A. P. Voitovich, L. P. Svirina, and V. N. Severikov, Dokl. Akad. Nauk BSSR, **33**, 978 (1989); A. P. Voitovich, L. P. Svirina, and V. N. Severikov, Opt. Commun. **80**, 435 (1991).
[16] L. P. Svirina, Opt. Commun. **111**, 370 (1994).
[17] G. P. Puccioni, M. V. Tratnik, J. E. Sipe, and G. L. Oppo, Opt. Lett. **12**, 242 (1987).
[18] P. Glorieux and A. Le Floch, Opt. Commun. **79**, 229 (1990).
[19] J. C. Cotteverte, F. B. Bretenaker, A. Le Floch, and P. Glorieux, Phys. Rev. A **49**, 2868 (1994).
[20] A. P. Voitovich, A. M. Kul'minskii, and V. N. Severikov, Opt. Commun. **126**, 152 (1996).
[21] L. P. Svirina, Opt. Spektrosk. **83**, 501 (1997) [Opt. Spectrosc. **83**, 473 (1997)].
[22] C. Serrat, R. Vilaseca, and R. Corbalan, Opt. Lett. **20**, 1353 (1995); E. Roldan, G. J. de Valcarcel, R. Vilaseca, and R. Corbalan, Phys. Rev. A **49**, 1487 (1994); A. M. Kul'minskii, R. Vilaseca, and R. Corbalan, Opt. Lett. **20**, 2390 (1995).
[23] J. Rendondo, E. Roldan, and G. J. de Valcarcel, Phys. Lett. A **210**, 301 (1996).
[24] W. E. Lamb, Phys. Rev. A **134**, 1429 (1964).
[25] R. C. Jones, J. Opt. Soc. Am. **31**, 408 (1941); **38**, 671 (1948); **46**, 126 (1956).
[26] H. I. Raterink, H. Under Stadt, C. H. F. Velzel, and G. X. Dijkstra, Appl. Opt. **6**, 813 (1967).
[27] M. SargentIII, W. E. Lamb, Jr., and R. L. Fork, Phys. Rev. **164**, 450 (1967).
[28] W. J. Tomlinson and R. L. Fork, Phys. Rev. **164**, 466 (1967).
[29] W. Van Haeringen, Phys. Rev. **158**, 256 (1967).
[30] D. Lenstra, Phys. Rep. **59**, 301 (1980).
[31] W. M. Doyle and M. B. White, Phys. Rev. **147**, 359 (1966).
[32] V. A. Zborovskii and E. Ye. Fradkin, Zh. Éksp. Teor. Fiz. **66**, 1219 (1974) [Sov. Phys. JETP **39**, 873 (1975)]; E. A. Tiunov and E. Ye. Fradkin, Kvant. Elektron (Moscow) **9**, 889 (1982) [Sov. J. Quantum Electron. **12**, 563 (1982)].
[33] J. Sjerve, P. Paddon, A. G. May, and G. Stephan, J. Opt. Soc. Am. B **12**, 440 (1995).
[34] V. S. Rubanov, L. P. Svirina, and V. N. Severikov, Dokl. Akad. Nauk BSSR **26**, 616 (1982); N. V. Iljushchenko, L. P. Svirina, and V. N. Severikov, Opt. Spektrosk. **54**, 380 (1983) [Opt. Spectrosc. **54**, 225 (1983)]; **54**, 874 (1983) [**54**, 517 (1983)]; V. M. Kuznetsov, V. S. Rubanov, L. P. Svirina, and V. N. Severikov, Kvant. Elektron. (Moscow) **13**, 66 (1986) [Sov. J. Quantum Electron. **16**, 38 (1986)]; A. P. Voitovich and V. N. Severikov, *Lazery s Anizotropnymi Rezonatorami* (Nauka i Tekhnika, Minsk, 1988).
[35] E. Yu. Andreeva, K. D. Teryokhin, and S. A. Fridrikhov, Opt. Spektrosk. **27**, 441 (1969) [Opt. Spectrosc. **27**, 441 (1969)].
[36] M. A. Gubin, G. I. Kozin, and E. D. Protsenko, Opt. Spectrosk. **36**, 328 (1974) [Opt. Spectrosc. **36**, 287 (1974)].
[37] V. S. Smirnov and A. M. Tumaikin, Opt. Spektrosk. **40**, 1030 (1976) [Opt. Spectrosc. **40**, 593 (1976)].
[38] M. S. Borisova and I. P. Mazanko, Opt. Spektrosk. **47**, 126 (1979) [Opt. Spectrosc. **47**, 69 (1979)].
[39] Di Chen, E. Bernal, I. C. Chang, and G. N. Otto, IEEE J. Quantum Electron. **QE-6**, 259 (1970).
[40] L. P. Svirina, Opt. Spektrosk. **77**, 124 (1994) [Opt. Spectrosc. **77**, 110 (1994)].
[41] V. S. Anishchenko, *Slozhnye Kolebaniya v Prostykh Sistemakh* (Nauka, Moskwa, 1990).
[42] P. Azzam and N. Bashara, *Ellipsometry and Polarized Light* (North-Holland, Amsterdam, 1977).
[43] E. Roldan, G. J. de Valcarcel, R. Vilaseca, and P. Mandel, Phys. Rev. A **48**, 591 (1993).
[44] V. Yu. Toronov and V. L. Derbov, Phys. Rev. A **50**, 878 (1994).
[45] *Volnovye i Fluktuatsionnye Protsessy v Lazerakh*, edited by Yu. L. Klimontovich (Nauka, Moscow, 1974).